Hydrogen Absorption of Incoherent TiC Particles in Iron from Environment at High Temperatures

F.G. WEI and K. TSUZAKI

The effect of atmosphere in heat treatment on the hydrogen trapping of incoherent TiC particles in iron has been studied in order to clarify the origin of hydrogen trapped by incoherent TiC particles. The hydrogen trapped by incoherent TiC particles in iron after austenitizing and tempering treatments in air, in a nonprotective argon atmosphere, and in an ultrahigh vacuum (UHV) was identified and quantitatively measured by thermal-desorption spectrometry (TDS). Results showed that incoherent TiC particles in iron do not trap hydrogen at ambient temperature by a cathodic-charging method. It was justified that incoherent TiC particles trap hydrogen during high-temperature heat treatment in nonprotective atmospheres. The amount of hydrogen trapped by incoherent TiC particles decreases with increasing heat-treatment temperature, which is well explained by the equilibrium concentration of hydrogen trapped by incoherent TiC particles in iron under an atmosphere containing water vapor. The hydrogen is supplied through water-vapor oxidation of iron at high temperatures. According to this model, a binding energy between hydrogen and incoherent TiC of 53 kJ/mol was obtained. The energy barrier for hydrogen to jump into incoherent TiC was determined to range from 21 to 35 kJ/mol, which is too high for hydrogen to be trapped by incoherent TiC at low temperatures.

I. INTRODUCTION

HYDROGEN diffusing in an iron lattice is likely absorbed by certain kinds of microstructural inhomogeneities that act as hydrogen traps, such as vacancies; impurity elements; dislocations; grain-boundary, precipitate/ferrite, and inclusion/ferrite interfaces; *etc*.[1] Many data on the hydrogen/trap interaction energy have been documented in the literature.[1,2,3] Incoherent TiC particles in steel are known to be a strong hydrogen trap with a high interaction energy of 95 kJ/mol, as reported by Pressouyre and Bernstein[4] by means of the electrochemical permeation method, or of 87 kJ/mol, as reported by Lee and Lee[5] by means of thermal-desorption spectrometry (TDS) analysis. The interaction energy is so high that once hydrogen is trapped, it cannot be released unless it is heated to high temperatures.

In spite of a number of data on the hydrogen-trapping properties of a variety of traps, little is known about the effect of heat treatment on the trapping property. Pressouyre[6] suggested that the increase in coherency of TiC precipitates with the ferrite matrix makes it more reversible in trapping nature. Lee and Lee[7] found that annealing temperature and time significantly influence the amount of hydrogen trapped by incoherent TiC and the temperature of the maximum hydrogen desorption rate. Recently, the present authors[8] found that incoherent TiC particles in 0.42C-0.30Ti steel demonstrate a variable hydrogen-trapping capability; they trapped the most hydrogen when tempered at 500 °C, and the hydrogen amount decreased with increasing tempering temperature above 500 °C with a concomitant increase in the temperature of the desorption peak. Moreover, it was further found by the present authors that, accompanying the change in the absorbed-hydrogen amount and peak temperature, the activation energy for desorption of hydrogen from incoherent TiC particles increases with increasing tempering temperature, presumably due to the chemical change at the particle/ferrite interface.[9] Besides the tempering temperature and time, the heat-treatment atmosphere may influence the hydrogen-trapping property. However, almost no attention has been paid, to date, to the effect of heat-treatment-atmosphere environment on the hydrogen trapping in iron and steel. Huang *et al*.[10] found that oxygen from the atmosphere segregates to Pd/MgO and Pd/Al_2O_3 interfaces in Pd-based alloys when annealed in air, and the excess oxygen traps hydrogen in the subsequent hydrogen-charging process. Annealing in vacuum or in metal vapor removed the excess oxygen from the interface, and no hydrogen trapping was observed. Oxygen segregation has been found in other noble metal/oxide interfaces.[11,12] These results indicate that atmosphere may play an important role in hydrogen trapping. Since heat treatment of iron and steel is usually performed in an atmosphere containing oxygen, the possibility of oxygen-assisting hydrogen absorption is also examined in the present study.

Because of the high interaction of incoherent TiC with hydrogen, it was often taken for granted in the past literature that incoherent TiC particles trap hydrogen prior to other weak traps in hydrogen-permeation measurements at room temperature. In a preliminary experiment, however, we found that incoherent TiC particles in iron already trapped hydrogen before hydrogen charging at room temperature. It is obvious that hydrogen had been introduced into the sample from the environment. The principal purpose of the present work was, then, to identify the origin of hydrogen that was trapped by incoherent TiC particles. The effects of heat-treatment atmospheres and also of the cooling medium on the hydrogen-trapping property of incoherent TiC particles were investigated by conducting heat treatment in nonprotective atmospheres and in ultrahigh vacuum (UHV) with different cooling media.

F.G. WEI, Postdoctoral Fellow, and K. TSUZAKI, Deputy Director-General, are with the Steel Research Center, National Institute for Materials Science, Tsukuba, Ibaraki 305-0047, Japan. Contact e-mail: fugao.wei@nims.go.jp

Manuscript submitted December 11, 2003.

II. EXPERIMENTAL DETAILS

A. *Material and Heat Treatments*

The material for study is high-purity iron with additions of nominal 0.05 wt pct carbon and 0.20 wt pct titanium in the TiC stoichiometric ratio and 2.0 wt pct nickel. The chemical composition is shown in Table I. The material was supplied in hot-rolled plates of 30 mm in thickness. Cylindrical specimens for heat treatment, of 10 mm in diameter and 100 mm in length, were manufactured from the plates. Two basic kinds of heat-treatment atmospheres had been adopted for investigation. One is the usual procedure we adopted in previous work:[8,9] in an argon atmosphere. The austenitizing treatment was designed at the relatively low temperature of 950 °C in order to obtain, as much as possible, incoherent TiC particles in the ferrite matrix. According to the Thermo-Calc calculation result, about 83 pct of the total 0.43 vol pct TiC will remain undissolved in austenite at 950 °C. The remaining 17 vol pct of TiC will precipitate in ferrite during the subsequent tempering heat treatment. After austenitizing at 950 °C for 15 minutes, the specimens were ice-brine quenched (IBQ), and some of the specimens were further tempered at 600 °C or 800 °C for 3 hours and water cooled (WC). Owing to the furnace structure, the argon atmosphere in our experiment could not shield the samples from being oxidized, but only alleviated the extent of oxidation, *i.e.*, the argon atmosphere in this study was nonprotective or only partially protective. Heat treatment in the argon atmosphere resulted in the formation of oxide scales on the specimens.

The other heat-treatment atmosphere is UHV. Heat treatment in UHV was conducted in the desorption spectrometer that was mainly used for hydrogen-desorption analysis in the present study. The total pressure in the analysis chamber of the spectrometer was about 1×10^{-7} Pa at room temperature. Vacuum treatment was carried out by heating specimens to 950 °C at a heating rate of 600 °C/h, holding for 15 minutes, then rapidly cooling by switching off the power, opening the heating furnace, and cooling by a fan (the specimen was still in vacuum). The cooling rate was measured by impinging a thermocouple into the center of the specimen to be 30 °C/min to 50 °C/min at temperatures above 500 °C. When further heat treatment in argon after the vacuum treatment was not necessary, cylindrical specimens for TDS analysis of 5 mm in diameter and 40 min in length were adopted and directly heat treated or degassed in vacuum. However, for those requiring further heat treatment in argon after the vacuum treatment, bigger specimens of 10 mm in diameter and 100 mm in length were used, and the holding time at 950 °C was 45 minutes.

Additionally, plate specimens of dimensions of about $30 \times 13 \times 2$ mm^3 were used to study the effects of water cooling and air cooling on hydrogen trapping, because plate specimens could be easily surface ground to avoid long-time exposure in air before TDS analysis. The time of exposure in air was less than 1 hour. Tempering treatments in air at 600 °C and 800 °C, followed by air cooling of degassed specimens at 950 °C, were also done with the same plate specimens. In the case of air cooling, the plate specimen was ground in a dry condition without water contact and was cleaned with acetone.

B. *Hydrogen Charging and TDS Analysis*

The dimensions of all cylindrical specimens for TDS analysis were 5 mm in diameter and 40 mm in length. For those that needed hydrogen charging, they were cathodically charged under the same charging condition except for the charging time. The charging solution was a 3 wt pct NaCl aqueous solution with an addition of 0.3 wt pct NH_4SCN. The charging current was kept at 0.1 mA/cm^2. The charging times were 1, 48, and 96 hours. Our preliminary result showed that the material used in the present study is saturated with hydrogen when the charging time is over 48 hours. The specimens charged for 1 hour were immediately electroplated with cadmium after charging and were held at room temperature for 48 hours for hydrogen homogenization before TDS analysis. The cadmium layer was removed by the electrolytic method before TDS analysis. Details of electroplating and removal of the cadmium layer can be found in Reference 9. Specimens that were charged over 48 hours were directly moved into the spectrometer for hydrogen analysis. Specimens that did not need charging were also polished electrolytically to obtain a clean surface before TDS analysis. The TDS analysis was conducted at a constant heating rate of 100 °C/h, and hydrogen was analyzed by a quadrupole mass spectrometer. A blank run without a sample was performed to obtain the background hydrogen, and the hydrogen TDS curves given in the present study have been subtracted from the background hydrogen level. Hydrogen trapped by a certain kind of trap was calculated by integrating the area under the desorption peak corresponding to the trap.

Plate specimens for studying the effects of cooling media and heat treatment in air were not charged with hydrogen by the cathodic method. The experimental condition of TDS analysis was identical to that for the cylindrical specimens.

The desorption rate of oxygen was measured simultaneously with hydrogen for some specimens. Before TDS measurement, tuning of the oxygen and hydrogen mass peaks was done and desorption rates of oxygen and hydrogen were calibrated, respectively, with pure oxygen and hydrogen standard gas cylinders, for which the leak rates were known.

C. *Measurement of Hydrogen-Desorption Activation Energy*

The activation energy for desorption of hydrogen from trap sites was determined by fitting the desorption kinetic formula (Eq. [1]) to the experimental spectrum by adjusting the constant (A) and the desorption activation energy (E_d).[9]

$$dX/dt = A(1 - X) \exp(-E_d/RT) \qquad [1]$$

where X is the fraction of hydrogen having left the specimen, t is the time, R is the gas constant, and T is the absolute temperature.

Table I. Chemical Composition of the Material Used, in Weight Percent

C	Ti	Ni	Si	Mn	P	S	N	O	Fe
0.051	0.22	1.99	<0.01	<0.01	<0.003	0.0008	0.0015	0.0012	bal

D. *Microstructure Characterization*

The microstructures were observed by means of transmission electron microscopy (TEM). The dark-field technique was used for imaging the relatively coarse incoherent TiC particles. High-resolution TEM (HRTEM) was employed to image the fine TiC precipitates. The TEM foils were prepared by mechanical thinning and electrolytic polishing in perchloric acid methanol solution at −50 °C. The TEM observation was carried out on a JEOL* JEM-2010F field-emission transmission electron microscope operating at 200 kV.

*JEOL is a trademark of Japan Electron Optics Ltd., Tokyo.

III. RESULTS

A. *Microstructures*

Figure 1 shows the dark-field images of incoherent TiC particles in the as-quenched sample and those tempered at 600 °C and 800 °C. No significant difference has been found among the three specimens with regard to the size and distribution of incoherent TiC particles. All the quenched and tempered samples contain a large number of fine particles with a diameter of about 20 nm, among which some larger particles of about 120 nm in diameter co-exist. A small part of TiC particles dissolved in austenite at 950 °C and precipitated in ferrite during the subsequent tempering treatment. Figure 2 gives the HRTEM images of the TiC precipitates. Fine coherent TiC platelets precipitate in the ferrite at 600 °C, as shown in Figure 2(a), with a habit plane on the ferrite (100) plane (the coherent plane) and holding the Baker–Nutting orientation relationship[13] with the ferrite matrix, *i.e.*, $(100)_{TiC}//(100)_{ferrite}$ and $[011]_{TiC}//[001]_{ferrite}$. The crystallography and morphology of the coherent TiC particles are described elsewhere in more detail.[14] Tempering at 800 °C promoted coarsening of the precipitates and removed them from the microstructure (Figure 2(b)). For this reason, it is difficult to differentiate the newly precipitated TiC particles from those that were present before tempering at 800 °C. Diffraction analysis indicated that the precipitate in Figure 2(b) obeys an orientation relationship with the ferrite matrix noticeably deviating from the Baker–Nutting one.

B. *Hydrogen Desorption of the Samples Heat Treated in Nonprotective Argon Atmosphere*

The desorption spectra with and without hydrogen precharging for the samples quenched and tempered in argon atmosphere are shown in Figure 3 (the desorption spectrum in this article refers to the hydrogen-desorption spectrum if without special indication, and the parts-per-million unit of hydrogen content refers to weight parts per million). It was justified, from the relation between the peak height and change in microstructure, that the desorption peak appearing around 620 °C corresponds to the hydrogen being released from incoherent TiC and that at 220 °C corresponds to the hydrogen from the interface between coherent TiC precipitates and the ferrite matrix. The peak associated with the dislocation and grain boundary (they are not distinguishable in the present study) is located between 95 °C and 180 °C, depending on tempering temperature. It approaches the peak of the coherent TiC/ferrite interface in the sample tempered at 600 °C (Figure 3(b)), the temperature corresponding to the early stage of TiC precipitation. The coherent TiC/ferrite interface showed a high hydrogen capacity when tempered at 600 °C due to the largest area

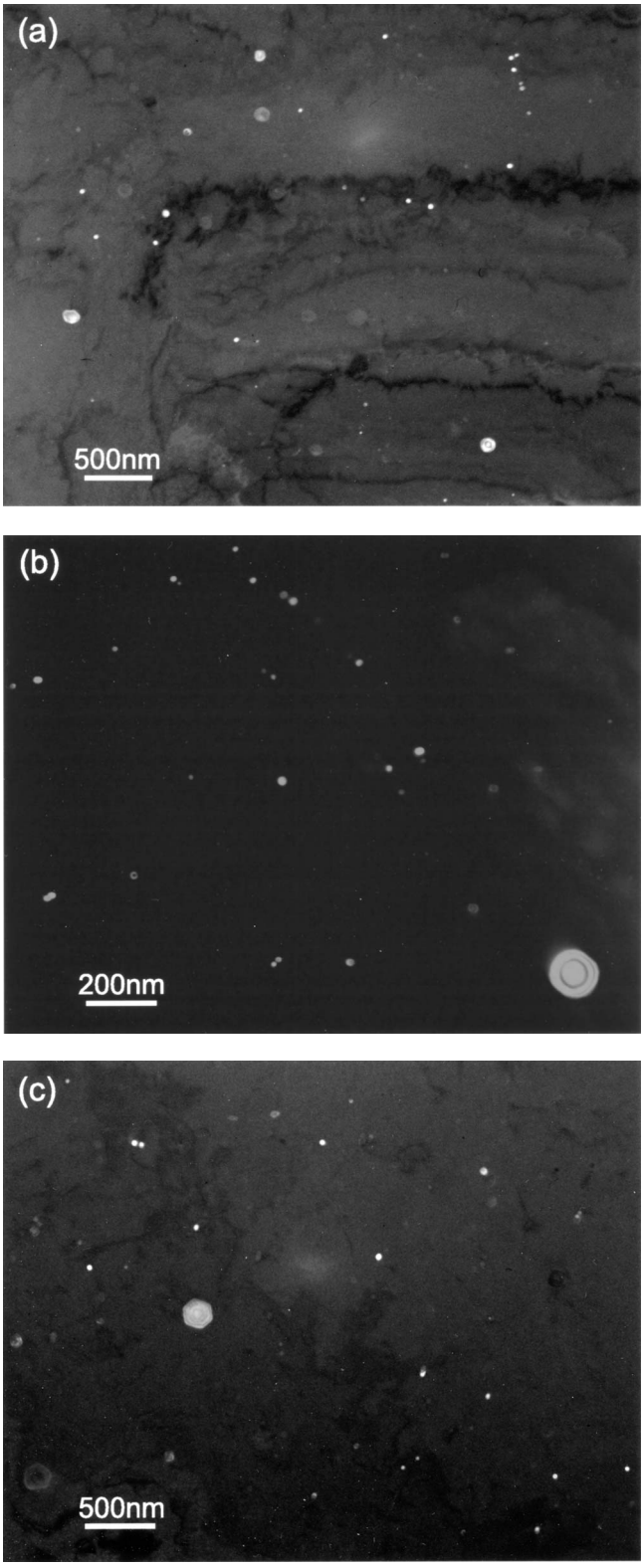

Fig. 1—Dark-field TEM micrographs showing the incoherent TiC particles in the samples (*a*) austenitized at 950 °C for 15 min, (*b*) tempered at 600 °C, and (*c*) at 800 °C for 3 h.

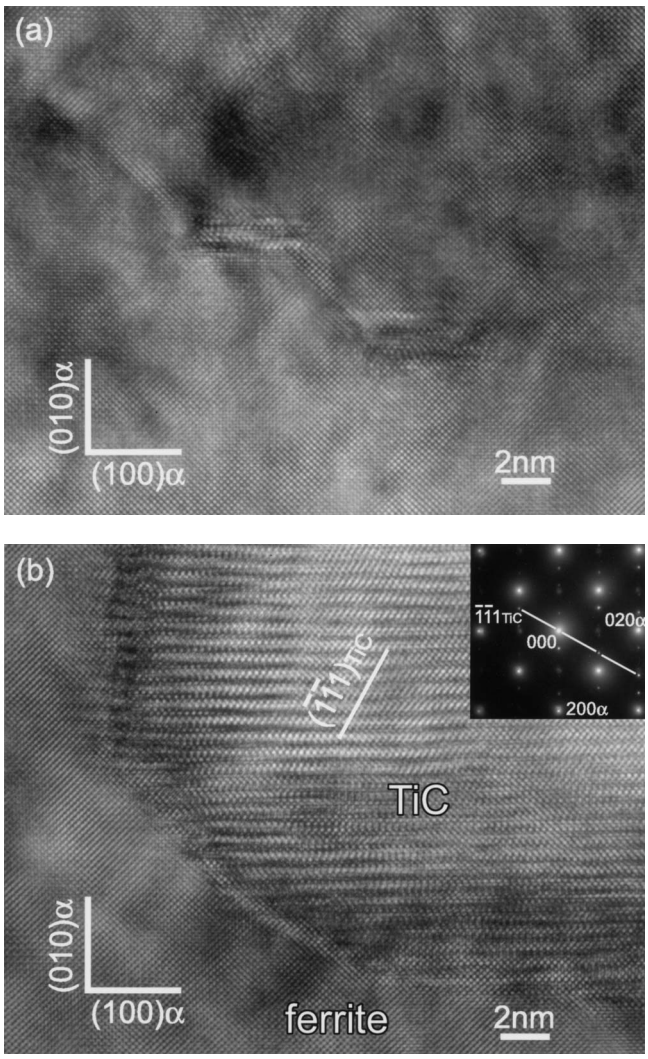

Fig. 2—High-resolution TEM micrographs showing (*a*) coherent TiC precipitates in the ferrite matrix in the sample tempered at 600 °C and (*b*) coarsened TiC precipitate in the sample tempered at 800 °C.

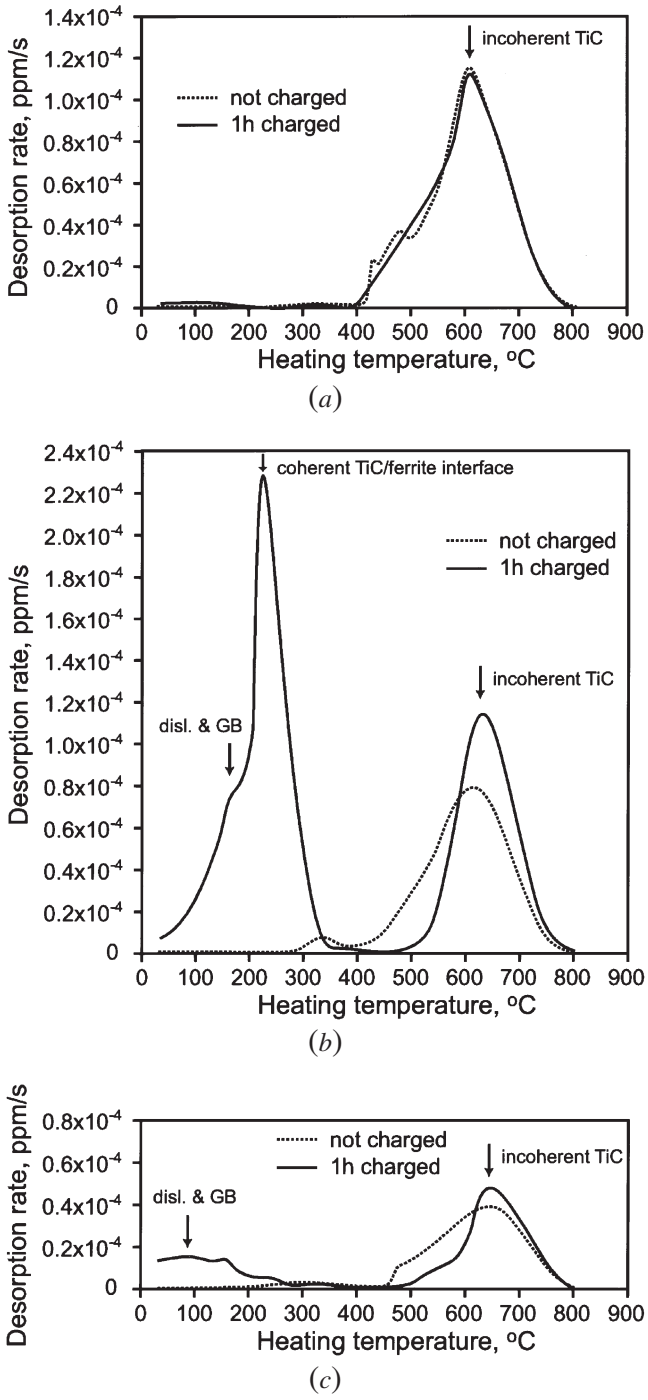

Fig. 3—TDS spectra of the samples heat treated in argon with and without hydrogen charging at room temperature: (*a*) austenitized at 950 °C for 15 min, (*b*) tempered at 600 °C, and (*c*) at 800 °C for 3 h.

of coherent interface. The hydrogen-trapping behavior of the coherent TiC/ferrite interface is another subject of our investigation.[15] Although the grain boundary, dislocation, and coherent TiC particles are also important traps, this article only focused on the incoherent TiC particles. As can been seen in Figure 3, these kinds of traps do not trap hydrogen before cathodic hydrogen charging, which is different from the incoherent TiC particles described subsequently.

It is surprising that almost no change was found between the desorption peaks of incoherent TiC particles with and without hydrogen charging in the as-quenched sample (Figure 3(a)). Similar phenomena are found in the 600 °C and 800 °C tempered samples, although the amount of hydrogen trapped by incoherent TiC decreases as the tempering temperature increases (Figures 3(b) and (c)). Obviously, hydrogen had been absorbed by incoherent TiC before charging. To explain the origin of the trapped hydrogen, two possibilities are considered. One is that oxygen dissolved in the sample during heat treatment and assisted absorption of hydrogen at ambient temperature from the environment, in the way like Huang *et al.*[10] suggested. The other possibility is that hydrogen has already been absorbed by incoherent TiC particles during heat treatment. To examine the first possibility, oxygen-desorption rates in the sample quenched from 950 °C and the samples tempered at 600 °C and 800 °C in argon were measured. Three samples gave similar oxygen desorption rates, and the result for the 600 °C tempered sample is shown in Figure 4. Only a small peak of the oxygen desorption rate is found at 320 °C. The small peak corresponds to 0.0015 ppm oxygen. Since the height of this oxygen peak becomes larger if cleaning of the sample surface

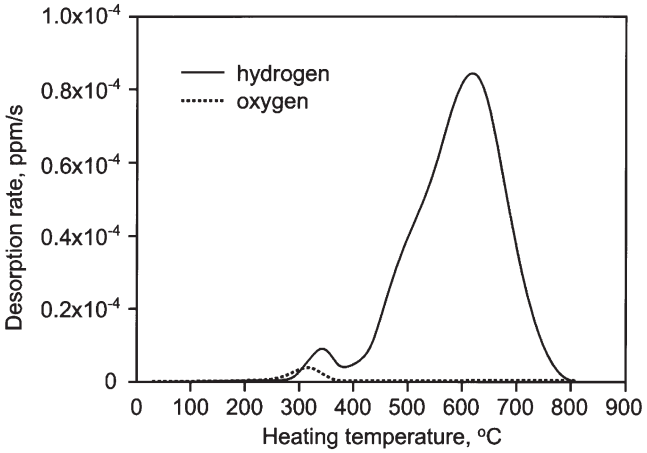

Fig. 4—Oxygen and hydrogen desorption rates for the sample austenitized at 950 °C for 15 min and tempered at 600 °C for 3 h in argon.

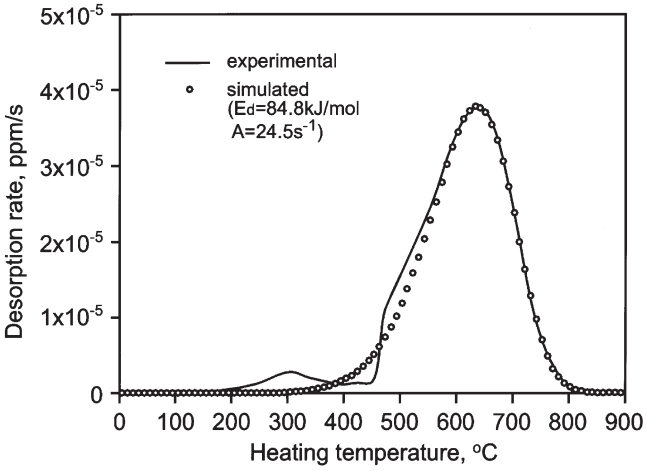

Fig. 5—Determination of desorption activation energy by fitting Eq. [1] to the experimental TDS spectrum for the sample tempered at 800 °C without hydrogen charging.

is not complete, it is believed that this oxygen comes from contamination of the sample surface. Therefore, the hydrogen trapping of incoherent TiC particles cannot be explained by oxygen assistance. The second possibility to account for hydrogen trapping of incoherent TiC particles is that, during heat treatment at high temperatures, hydrogen trapping occurred from the environment. Identification of a specific stage in the heat treatment will be described using predegassed samples in Section III–E.

An example of measuring the desorption activation energy by fitting Eq. [1] to the TDS spectrum is given in Figure 5 for the sample tempered at 800 °C without hydrogen charging. The best fit yields a desorption activation energy of 84.8 kJ/mol. This value is close to the value of 87 kJ/mol reported by Lee and Lee,[5] who measured it by changing the heating-rate method in TDS analysis for a 0.5C-2.0Ti steel annealed at 700 °C for 24 hours and precharged with hydrogen in hydrogen gas at 400 °C for 3 hours. However, the activation energy is a little bit smaller than the value of 95 kJ/mol measured by Pressouyre and Bernstein[4] by the electrochemical permeation method for incoherent TiC–containing iron annealed at 800 °C under an unspecified atmosphere. It is worth noticing, in Figure 5, a small deviation of the experimental desorption curve from the calculated spectrum on the low-temperature side with respect to the peak temperature, while a good match can be seen on the high-temperature side.

The amount of hydrogen trapped by incoherent TiC and the desorption activation energy are summarized in Table II, together with the data obtained in Sections III–C and III–D. The activation energies are plotted against the final heat-treatment temperature, as shown in Figure 6. There is a trend that when the final heat-treatment temperature increases, the hydrogen amount decreases while the desorption activation energy increases. It should be pointed out that incoherent TiC particles in the as-received sample already absorbed an average of 0.8752 ppm hydrogen before heat treatment. The austenitizing time of 15 minutes at 950 °C is not long enough for hydrogen to reach its equilibrium, and a high amount of hydrogen was retained in the 950 °C × 15 min as-quenched sample.

Table II. Effect of Heat Treatment on the Amount of Hydrogen Trapped by Incoherent TiC and the Activation Energy for Hydrogen Desorption

Final Heat-Treatment Temperature	Heat Treatment	Charging Condition	Hydrogen Content (ppm)	Activation Energy (kJ/mol)
950 °C	950 °C × 15 min IBQ as-quenched	not charged	0.6960*	—
		1 h charged	0.6874*	—
	950 °C × 3 h IBQ as-quenched	not charged	0.2905	87.3**
	950 °C × 45 min (in vacuum) +	not charged	0.1236	87.7**
	950 °C × 3 h WC	1 h charged	0.1430	—
600 °C	950 °C × 15 min IBQ +	not charged	0.5142	78.7
	600 °C × 3 h WC	1 h charged	0.5340	77.3**
	950 °C × 45 min (in vacuum) +	not charged	0.4095	74.0
	600 °C × 3 h WC	1 h charged	0.4943	74.0
800 °C	950 °C × 15 min IBQ +	not charged	0.2606	84.8
	800 °C × 3 h WC	1 h charged	0.2288	84.8**
	950 °C × 15 min IBQ +	not charged	0.1626	84.8
	800 °C × 3 h IBQ + 800 °C × 3 h WC			

*Not equilibrium value.
**Less satisfactory fit to the low-temperature side of the desorption peak.
Remark: the average amount of hydrogen absorbed by incoherent TiC in the as-received sample was 0.8752 ppm on average.

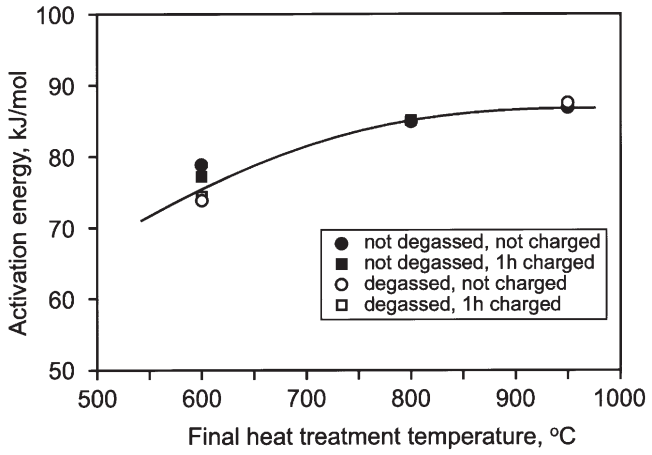

Fig. 6—Final heat-treatment temperature dependence of activation energy for hydrogen desorption from incoherent TiC particles in samples with and without hydrogen degassing (vacuum treatment at 950 °C) and charging. Data are taken from Table II.

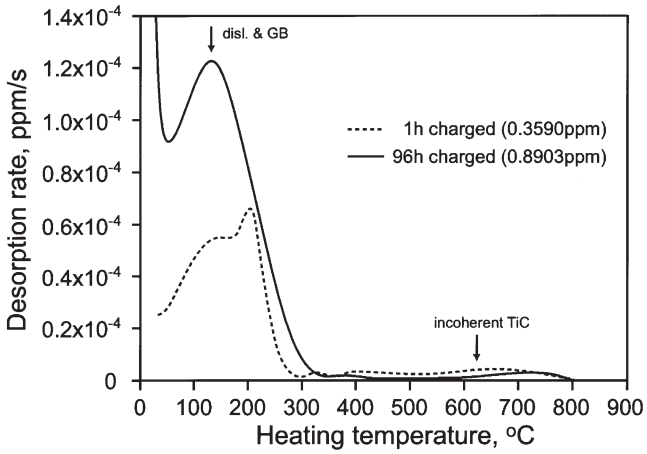

Fig. 7—TDS spectrum for the sample degassed at 950 °C for 15 min in vacuum and hydrogen charged at room temperature for 1 and 96 h, respectively. The mounts of hydrogen trapped by grain boundary and dislocation (peak below 300 °C) for different charging times are indicated.

C. *The TDS Spectra after Vacuum Heat Treatment*

Heat treatment (600 °C/h heated to 950 °C and held for 15 minutes) in UHV in the desorption spectrometer eliminated the incoherent TiC peak, even though the sample was charged for 96 hours. This is illustrated in Figure 7. Only a little residual hydrogen was detected above 400 °C, where the desorption peak of incoherent TiC particles should have been located. Increasing the charging-current density by 10 times (1 mA/cm^2) was insufficient to introduce hydrogen into incoherent TiC particles. This result indicates that incoherent TiC particles in iron do not trap hydrogen at room temperature, even though the sample is cathodically charged.

In contrast to incoherent TiC particles, vacuum treatment obviously increases the amount of hydrogen trapped by the coherent TiC/ferrite interface, dislocation, and grain boundary, because the low-temperature peak at about 150 °C in Figure 7 is much higher than that found in Figure 3(a) for heat treatment in argon followed by water quenching. It was determined (not shown here) that the saturation hydrogen content associated with the low-temperature peak is only 0.0809 ppm in the case of heat treatment in argon, which is much lower than the saturation value of 0.8903 ppm in vacuum treatment. The difference can be rationalized by the change in microstructure or chemistry, such as segregation of some kind of impurity during the slower cooling process after vacuum treatment. Justification of this needs further investigation.

Since tempering treatment may alter the quantity of hydrogen trapped by incoherent TiC, as shown in Figure 3, an experiment of cyclic vacuum heat treatment and TDS analysis using a single sample, as shown in Figure 8, was designed to examine the effect of tempering temperature on hydrogen absorption. Spectrum TDS0 is taken from Figure 3(c) or Figure 5 for the uncharged 800 °C tempered sample. All TDS analyses were conducted at the same heating rate of 100 °C/h, and the subsequent 3-hour holding at 800 °C and 600 °C in vacuum was followed by a rapid cooling by opening the furnace. Spectra TDS1 through TDS 3 were measured by the same sample. The fact that spectrum TDS1 shows a lower peak at 620 °C than TDS0 indicates that an additional 3 hours of tempering at

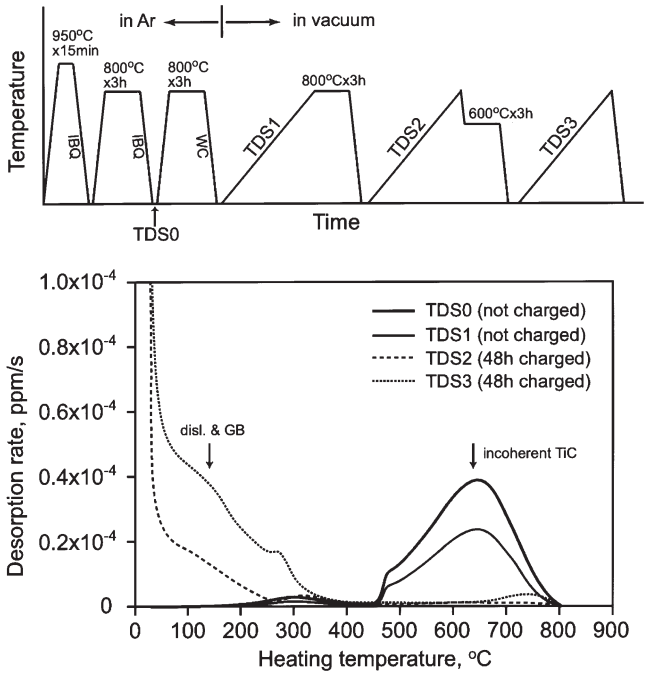

Fig. 8—Effect of tempering temperature in vacuum heat treatment on the hydrogen trapping of incoherent TiC particles and other traps in cathodic charging at room temperature. TDS spectra (TDS1 ~ 3) were obtained using the same sample. TDS0 is taken from Fig. 3(c) for comparison.

800 °C in argon decreases the amount of hydrogen trapped by incoherent TiC to some extent. After 3 hours of holding at 800 °C in vacuum after TDS1 analysis, even charging for 48 hours at room temperature cannot restore hydrogen absorption (TDS2), in agreement with the result of the sample vacuum heat treated at 950 °C (Figure 7). Spectrum TDS3 after holding at 600 °C demonstrates the same result. It is concluded that incoherent TiC particles in iron do not trap hydrogen at all at room temperature.

However, some noticeable change can be seen in the effect of tempering temperature on hydrogen trapping of the grain

boundary and dislocation in Figure 8 (the coherent TiC precipitate is absent after 800 °C tempering). Tempering at 600 °C (TDS3) shows a higher content (0.5374 ppm) of hydrogen trapped by the dislocation and grain boundary than that tempered at 800 °C (TDS2) (0.2199 ppm). The change in dislocation density cannot account for this result, because additional tempering at 600 °C should result in a decrease in dislocation density. The change in chemistry, such as segregation of impurities at the dislocation and grain boundary, is possibly responsible for this enhancement in hydrogen absorption at 600 °C.

D. *Reversibility of Hydrogen Trapping of Incoherent TiC Particles*

Rod samples of 10 mm in diameter and 100 mm in length were used for this investigation, and they were first heated to 950 °C at a rate of 600 °C/h and held for 45 minutes in the desorption spectrometer for complete release of hydrogen. After hydrogen degassing, the samples were subjected to 950 °C and 600 °C, respectively, for 3 hours in argon, followed by water cooling. Results of TDS analysis for both samples are shown in Figure 9. During heat treatments at 950 °C and 600 °C in argon, the incoherent TiC particles in degassed samples absorb hydrogen again, regardless of whether the samples were charged or not. The amounts of hydrogen trapped by incoherent particles and the desorption activation energies calculated from these spectra are added to Table II. Both the hydrogen content and activation energy are consistent with those obtained from the samples that did not receive degassing treatment. The higher amount of hydrogen in the sample austenitized at 950 °C for 15 minutes results from incomplete outgassing of hydrogen that was inherited from the as-received state, and, thus, this value does not represent the equilibrium concentration of hydrogen at 950 °C.

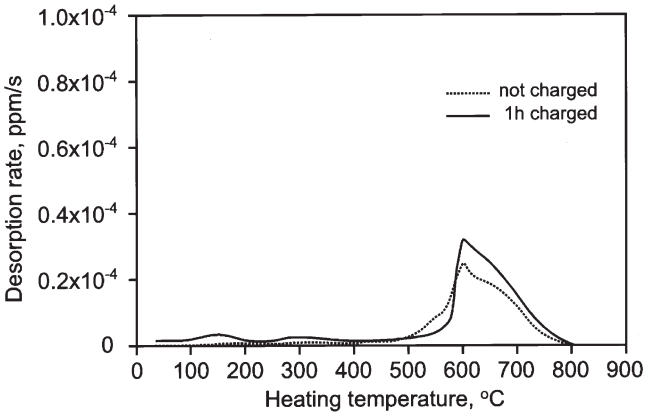

Fig. 9—TDS spectra for samples heat treated in argon at (*a*) 950 °C for 3 h and (*b*) 600 °C for 3 h after vacuum degassing at 950 °C for 45 min.

E. *Identification of When Hydrogen Was Trapped by Incoherent TiC Particles during Heat Treatment*

Plate specimens were prepared to specify at which stage in heat treatment hydrogen was absorbed. Because water cooling was adopted in the heat treatment, it was considered possible for hydrogen to enter the sample through water decomposition during water cooling. This possibility was ruled out, because air cooling of a degassed sample after tempering in argon at 600 °C for 3 hours resulted in the same TDS spectrum as that obtained with a water-cooled sample (Figure 9(b)). It is concluded that incoherent TiC particles absorbed hydrogen during heat treatment (tempering or austenitizing) at high temperatures. More specifically, the hydrogen trapped by incoherent TiC particles came from a certain kind of hydrogen source in air, not from a possible hydrogen-gas impurity contained in the argon atmosphere, since tempering at 600 °C in air also yielded a similar TDS curve, shown in Figure 9(b). In this sense, it is easy to understand that hydrogen absorbed by incoherent TiC in the as-received sample was probably introduced during hot rolling before reception.

IV. DISCUSSION

A. *Source of the Hydrogen Trapped by Incoherent TiC Particles and Thermodynamics of Hydrogen Absorption in Iron*

Since it is evident that the hydrogen trapped by incoherent TiC particles at high temperatures comes from the air environment, two kinds of gaseous hydrogen-containing components in air are considered to feed the incoherent TiC with hydrogen. One is the hydrogen gas, and the other is water vapor. Extremely dilute hydrogen gas in air is not energetically favorable to dissolve in iron when compared with the water vapor, and it is ruled out as a hydrogen source. Water vapor is probably the hydrogen source of incoherent TiC particle trapping at high temperatures in terms of the following thermodynamic consideration.

When iron is exposed to air at high temperatures, it is likely to be oxidized by oxygen and also by the water vapor. Hydrogen trapping of incoherent TiC in iron in air at high temperatures can be described as such a process: iron is oxidized by water vapor, which yields hydrogen gas, and the hydrogen gas dissolves as hydrogen atoms in the iron bulk beneath the oxide scale before it is finally trapped by TiC particles. This is schematically illustrated in Figure 10. The oxidation products of iron are composed of FeO (wustite), Fe_3O_4 (magnetite), and Fe_2O_3 (hematite), with FeO adjacent to the iron bulk substrate and Fe_2O_3 forming the outmost layer of the oxide scale.[16] For the case of water-vapor oxidation

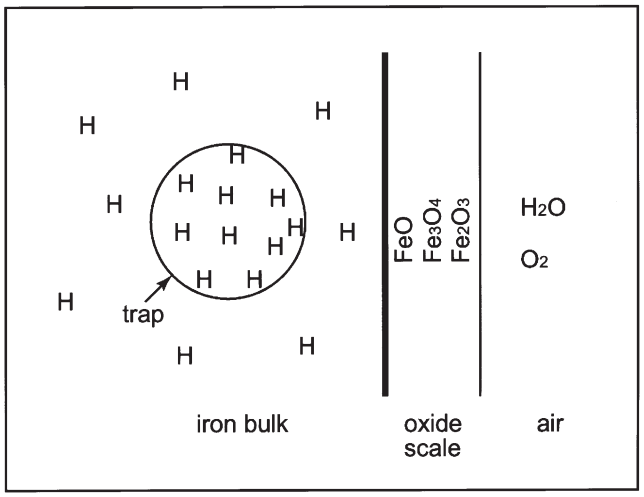

Fig. 10—Schematic illustration of generation of the hydrogen trapped by incoherent TiC particles in iron through surface reaction of iron sample in air at high temperatures.

yielding FeO, the possible reactions and their standard free energies[17] are

$$\text{Fe (s)} + \frac{1}{2}\text{O}_2\text{ (g)} = \text{FeO (s)}$$
$$\Delta G_1^0 = -259{,}600 + 62.55T\text{(J)} \quad [2]$$

$$\text{H}_2\text{ (g)} + \frac{1}{2}\text{O}_2\text{ (g)} = \text{H}_2\text{O (g)}$$
$$\Delta G_2^0 = -246{,}000 + 54.8T\text{(J)} \quad [3]$$

$$\frac{1}{2}\text{Fe (s)} + \frac{1}{2}\text{H}_2\text{O (g)} = \frac{1}{2}\text{FeO (s)} + \frac{1}{2}\text{H}_2\text{ (g)}$$
$$\Delta G_3^0 = \frac{1}{2}(\Delta G_1^0 - \Delta G_2^0) = -6800 + 3.88T\text{ (J/mol H)} \quad [4]$$

According to the Sievert's law of hydrogen solubility in pure iron, as suggested by Hirth,[1] based on the experiment of Quick and Johnson,[18]

$$C_L = 0.00185P_{\text{H}_2}^{1/2}\exp\left(-\frac{H_s}{\text{R}T}\right) \quad [5]$$

where C_L is the solubility, P_{H_2} is the hydrogen gas pressure (in atmospheric units), and H_s (equal to 28,620 J/mol H) is the heat of solution. The standard free energy for hydrogen dissolution is deduced to be

$$\frac{1}{2}\text{H}_2\text{ (g)} = [\text{H}] \qquad \Delta G_4^0 = 28{,}620 + 52.29T\text{ (J/mol H)} \quad [6]$$

where [H] denotes the hydrogen atom in iron. Then, the total reaction formula for absorption of hydrogen in iron through water-vapor oxidation and its standard free energy are

$$\frac{1}{2}\text{Fe (s)} + \frac{1}{2}\text{H}_2\text{O (g)} = \frac{1}{2}\text{FeO (s)} + [\text{H}]$$
$$\Delta G_5^0 = \Delta G_3^0 + \Delta G_4^0 = 21{,}790 + 56.16T\text{ (J/mol H)} \quad [7]$$

For the equilibrium reaction of Eq. [7], the solubility of hydrogen in iron under water-vapor pressure can be easily obtained:

$$C_L = 0.00116P_{\text{H}_2\text{O}}^{1/2}\exp\left(-\frac{21{,}820\text{ J/mol}}{\text{R}T}\right) \quad [8]$$

where $P_{\text{H}_2\text{O}}$ is the partial pressure of water vapor in air. Equation [8] indicates that the activation energy for hydrogen solution in pure iron is reduced by 6.80 kJ/mol H when the environmental atmosphere is changed from hydrogen gas to water vapor.

When the previous process is applied to the surface reaction, which yields Fe_3O_4 and Fe_2O_3, similar results can be available. The surface reaction, the standard free energy, and the hydrogen solubility can be expressed as follows:

for the case of Fe_3O_4,

$$\frac{3}{8}\text{Fe (s)} + \frac{1}{2}\text{H}_2\text{O (g)} = \frac{1}{8}\text{Fe}_3\text{O}_4\text{ (s)} + [\text{H}]$$
$$\Delta G_6^0 = 15{,}290 + 63.98T\text{ (J/mol H)} \quad [9]$$

$$C_L = 0.000453P_{\text{H}_2\text{O}}^{1/2}\exp\left(-\frac{15{,}290\text{ J/mol}}{\text{R}T}\right) \quad [10]$$

for the case of Fe_2O_3,

$$\frac{1}{3}\text{Fe (s)} + \frac{1}{2}\text{H}_2\text{O (g)} = \frac{1}{6}\text{Fe}_2\text{O}_3\text{ (s)} + [\text{H}]$$
$$\Delta G_7^0 = 116{,}550 + 67.22T\text{ (J/mol H)} \quad [11]$$

$$C_L = 0.000307P_{\text{H}_2\text{O}}^{1/2}\exp\left(-\frac{16{,}550\text{ J/mol}}{\text{R}T}\right) \quad [12]$$

It can be known from the previous thermodynamic analysis that, because of the greater reduction in activation energy compared to FeO, the formation of Fe_3O_4 and Fe_2O_3 is more energetically favorable for absorption of hydrogen in iron.

B. *Equilibrium Concentration of Hydrogen Trapped by Incoherent TiC Particles*

As demonstrated previously, the hydrogen concentration in pure iron at a certain temperature is determined by the pressure of the environmental water vapor. When traps are present in the iron, hydrogen in the normal iron lattice should be equilibrated with the environmental water vapor and the hydrogen at the traps simultaneously, as long as an equilibrium state is achieved. The trapped hydrogen (C_t) in equilibrium with that in the iron lattice can be obtained by Eq. [13], which was derived by Lee and Lee[19,20] on the basis of McNabb and Foster's[21] trap-and-release theory at equilibrium condition, but the hydrogen atmosphere is replaced by water vapor in the present case.

$$C_t = \frac{N_x\dfrac{C_0}{N_L}\exp\left(\dfrac{E_b - E_0}{\text{R}T}\right)}{1 + \dfrac{C_0}{N_L}\exp\left(\dfrac{E_b - E_0}{\text{R}T}\right)} \quad [13]$$

where N_x and N_L are the trap density and the normal iron-lattice interstitial-site density ($N_L = 5.26 \times 10^{29}$ sites/m^3), respectively; C_0 and E_0 are the coefficient and activation energy, respectively, in the expression of C_L ($C_L = C_0\exp(-E_0/\text{R}T)$) in Eqs. [5],

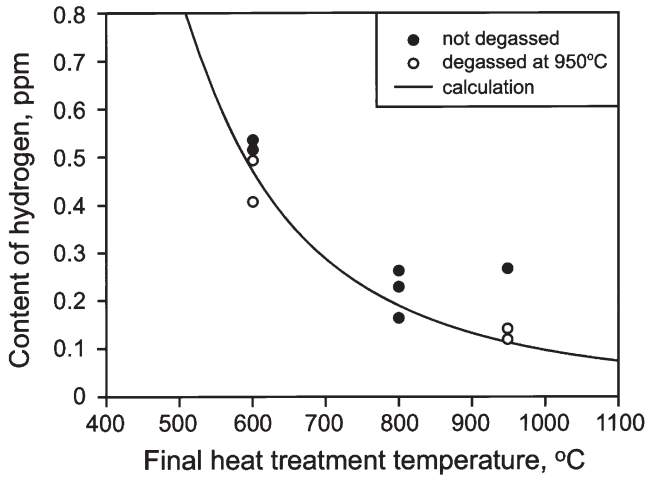

Fig. 11—Fitting Eq. [13] to the measured equilibrium content of hydrogen trapped by incoherent TiC particles. Hydrogen contents are taken from Table II.

[8], [10], and [12]; E_b is the binding energy of hydrogen with the trap; R is the gas constant; and T is the charging temperature (equivalent to the final heat-treatment temperature). The values of E_b and N_x can be determined by fitting Eq. [13] to the experimentally measured content of hydrogen trapped by incoherent TiC at different charging temperatures, provided that the partial pressure of water vapor in the atmosphere is known. This is shown in Figure 11. The data of hydrogen solubility are taken from Table II. Fe_3O_4 is taken as the product of oxidation, because it requires the smallest activation energy for dissolving hydrogen in iron. When the partial pressure of water vapor is taken to be 0.02 atm, a best fit to the experimental data gives a binding energy of 53 kJ/mol and a reasonable trap density of 2.37×10^{25} sites/m^3 that is equivalent to 5 ppm hydrogen in iron when the traps are saturated with hydrogen. The value of the binding energy is much higher than the value of 28.1 kJ/mol reported by Lee and Lee,[5] although the activation energy is comparable. With the binding energy, the barrier energy for trapping, *i.e.*, $E_d - E_b$, can be deduced from the data of activation energies summarized in Figure 6 or Table II. Then, it is known that the barrier energy for hydrogen trapping into incoherent TiC particles ranges from 21 to 35 kJ/mol, depending on the final heat-treatment temperature. The barrier energy is so high that hydrogen is difficult to jump into incoherent TiC particles at low temperatures, which explains why incoherent TiC particles cannot trap hydrogen at ambient temperature. Only at high temperatures, where thermal activation is sufficient, can incoherent TiC particles absorb hydrogen.

V. CONCLUSIONS

The origin of hydrogen trapped by incoherent TiC particles in iron has been clarified by hydrogen TDS study on an iron alloy containing 0.43 vol pct TiC particles after austenitizing at 950 °C and tempering at 600 °C and 800 °C in different atmospheres, *i.e.*, in nonprotective atmospheres and in vacuum. Some important conclusions can be drawn from the results obtained.

1. Incoherent TiC particles in iron do not trap hydrogen at ambient temperature, even if they are cathodically hydrogen charged for a long time. However, they trap hydrogen during heat treatments at 600 °C, 800 °C, and 950 °C in air and nonprotective argon atmosphere.
2. When the final heat-treatment temperature increases, the equilibrium amount of hydrogen trapped by incoherent TiC particles decreases while the activation energy for hydrogen desorption from the particles increases.
3. The hydrogen trapped by incoherent TiC particles was identified to be supplied through oxidation of iron by water vapor in the heat-treatment atmosphere. The equilibrium concentration of hydrogen trapped by incoherent TiC particles in iron at high temperatures can be well explained by the water-vapor oxidation model. According to this model, the binding energy of hydrogen with incoherent TiC particles and the trap density were determined to be 53 kJ/mol and 2.37×10^{25} sites/m^3, respectively.
4. The energy barrier for hydrogen trapping into incoherent TiC particles ranges from 21 to 35 kJ/mol. The energy barrier is so high that hydrogen cannot jump into incoherent TiC particles at low temperatures, which explains why incoherent TiC particles cannot trap hydrogen at room temperature.
5. No oxygen desorption was detected in TDS analysis up to 810 °C in the samples quenched from 950 °C and tempered at 600 °C and 800 °C in an argon atmosphere. As a result, oxygen takes no part in the hydrogen trapping of incoherent TiC particles, as well as coherent TiC precipitates, grain boundaries, and dislocations.
6. Coherent TiC precipitates, grain boundaries, and dislocations do not absorb hydrogen from the environment during heat treatment at high temperatures. However, they trap hydrogen at room temperature during cathodic charging, regardless of the thermal history and the type of atmosphere.

REFERENCES

1. J.P. Hirth: *Metall. Trans. A*, 1980, vol. 11A, pp. 861-90.
2. J.Y. Lee and S.M. Lee: *Surf. Coatings Technol.*, 1986, vol. 28, pp. 301-14.
3. I. Maroef, D.L. Olson, M. Eberhart, and G.R. Edwards: *Int. Mater. Rev.*, 2002, vol. 47, pp. 191-223.
4. G.M. Pressouyre and I.M. Bernstein: *Metall. Trans. A*, 1978, vol. 9A, pp. 1571-80.
5. H.G. Lee and J.Y. Lee: *Acta Metall.*, 1984, vol. 32, pp. 131-36.
6. G.M. Pressouyre: *Metall. Trans. A*, 1979, vol. 10A, pp. 1571-73.
7. S.M. Lee and J.Y. Lee: *Acta. Metall.*, 1987, vol. 35, pp. 2695-700.
8. F.G. Wei, T. Hara, T. Tsuchida, and K. Tsuzaki: *Iron Steel Inst. Jpn. Int.*, 2003, vol. 43, pp. 539-47.
9. F.G. Wei, T. Hara, and K. Tsuzaki: *Metall. Mater. Trans. B*, 2004, vol. 35B, pp. 587-97.
10. X.Y. Huang, W. Mader, and R. Kirchheim: *Acta Metall. Mater.*, 1991, vol. 39, pp. 893-907.
11. J. Gegner, G. Horz, and R. Kirchheim: *Interface Sci.*, 1997, vol. 5, pp. 231-43.
12. E. Pippel, J. Woltersdorf, J. Gegner, and R. Kirchheim: *Acta Mater.*, 2000, vol. 48, pp. 2571-78.
13. R.G. Baker and J. Nutting: *Precipitation Processes in Steels*, ISI Special Report, Iron and Steel Institute, London, 1959, vol. 64, pp. 1-22.
14. F.G. Wei, T. Hara, and K. Tsuzaki: *Phil. Mag.,* 2004, vol. 84, pp. 1735-51.
15. F.G. Wei and K. Tsuzaki: unpublished research.
16. K. Hauffe: *Oxidation of Metals*, Plenum Press, New York, NY, 1965, pp. 267-88.
17. D.R. Gaskell: *Introduction to Metallurgical Thermodynamics*, 2nd ed., Hemisphere Publishing Corporation, Washington, DC, 1981, pp. 585-86.
18. N.R. Quick and H.H. Johnson: *Acta Metall.*, 1978, vol. 26, pp. 903-07.
19. J.L. Lee and J.Y. Lee: *Metall. Trans. A*, 1986, vol. 17A, pp. 2183-86.
20. S.M. Lee and J.Y. Lee: *Metall. Trans. A*, 1986, vol. 17A, pp. 181-87.
21. A. McNabb and P.K. Foster: *Trans. TMS-AIME*, 1963, vol. 227, pp. 618-27.